Int. J. Heat Mass Transfer. Vol. 27, No. 9, pp. 1559–1571, 1984
Printed in Great Britain

0017-9310/84 $3.00 + 0.00

Effect of surface configuration on nucleate boiling heat transfer

KANEYASU NISHIKAWA, YASUNOBU FUJITA, SATORU UCHIDA
and HARUHIKO OHTA

Department of Mechanical Engineering, Kyushu University, Fukuoka, Japan

(*Received* 20 *December* 1983)

Abstract—To investigate in detail the effect of surface configuration on nucleate boiling heat transfer, the experiment of nucleate pool boiling of water at atmospheric pressure from a copper flat plate whose orientation is varied from 0° to 175° from the horizontal plane is performed. The effect of surface orientation is remarkable in the low heat flux region where the heat transfer coefficient increases as the inclination angle is increased. On the contrary there is no marked effect in the high heat flux region. To explain the observed effect of surface orientation for the surfaces facing downwards, two mechanisms of the sensible heat transport by compulsory removal of the thermal layer by the rising bubble and the latent heat transport by evaporation from thin liquid film underneath the rising bubble are proposed. The latter contribution becomes more predominant at large inclination angles.

1. INTRODUCTION

IN NUCLEATE boiling, the experimental data for heat transfer have usually been correlated according to the hypothesis that nucleate boiling is a localized process and the flow pattern near the heating surface has a dominant role in heat transfer. Furthermore, the heat transfer coefficient in nucleate boiling depends strongly on the condition of the heating surface. This fact makes it very difficult to correlate heat transfer in nucleate boiling. Therefore, such factors as shape, size, and configuration of the heating surface have been treated as secondary and their effects have been eliminated from the detailed considerations. It is partially due to the fact that there exists very limited information concerning these effects on nucleate boiling. As for the configuration of the heating surface, however, there seems to be observed considerable differences between the horizontal surface and the vertical surface in behavior such as the bubble generation, growth and detachment, the movement of bubbles and incidental liquid relative to the surface, the void fraction near the surface, and so on [1, 2]. And it may give rise to significant differences in heat transfer for these two configurations in turn. Consequently it becomes important to investigate in detail the effect of the configuration of the heating surface for the purpose of not only its technological implications but also the clarification of the mechanism in nucleate boiling.

The effects of surface orientation have been investigated under conditions of nucleate pool boiling by very few researchers. Jakob and Linke [3] performed the experiment of nucleate boiling of atmospheric water and carbon tetrachloride using two kinds of heating surfaces, a horizontal circular flat plate and a vertical cylinder. They concluded that there is no marked difference between the heat transfer coefficients for both surface configurations in nucleate boiling. Githinji and Sabersky [4] studied the effects of surface orientation in the subcooled nucleate boiling of isopropyl alcohol. They found that the boiling curve shifted upwards as the surface was changed from a horizontal facing upwards to a vertical position. However, when the heating surface was faced downwards the boiling curve shifted downwards below that for a horizontal surface facing upwards. Marcus and Dropkin [5] reported that the heat transfer coefficient in the nucleate boiling of water increased as the surface orientation was changed from a horizontal facing upwards to a vertical position. They noted that the nucleation sites were substantially decreased as the angle of inclination from the horizontal was increased. Class *et al.* [6] investigated both the effects of orientation and surface conditions in the boiling of liquid hydrogen. An upwards shift of the boiling curve was observed as the surface was changed from a horizontal to a vertical position for a smooth surface. For a greased surface, the shift occurred in the same direction but was more pronounced. When the smooth surface was roughened with emery paper, however, the shift occurred in the opposite direction. Upward shifts with an increase of inclination angle were observed also in the studies by Littles and Wallis [7] in the boiling of Freon 113, by Chen [8] in the boiling of Freon 11, by Vishnev *et al.* [9] in the boiling of Helium I and also by Jakob and Linke [3] in the boiling of water and carbon tetrachloride.

The purpose of this work is to present experimental data for heat transfer and bubble behavior on the flat surface at various orientations from a horizontal upwards to an almost horizontal downwards and to gain further information on the effect of surface configuration on heat transfer in nucleate boiling. Furthermore, a simple model for heat transfer in

NOMENCLATURE

a	thermal diffusivity [$m^2\ s^{-1}$]
$E(t_k)$	cumulative probability density function defined by equation (7)
$e(t_k)$	probability density function defined by equation (6)
f	void fraction
q	heat flux [$W\ m^{-2}$]
q_c	calculated heat flux by equation (8) [$W\ m^{-2}$]
q_l	time-averaged heat flux due to sensible heat transport [$W\ m^{-2}$]
q_M	measured heat flux [$W\ m^{-2}$]
q_v	time-averaged heat flux due to latent heat transport [$W\ m^{-2}$]
T	temperature [K]
T_{sat}	saturation temperature [K]
T_w	temperature of heating surface [K]
ΔT_{sat}	degree of superheat of heating surface [K]
t	time [s]
t_l	time period during which the heating surface is in contact with the bulk liquid [s]
$\overline{t_l}$	average value of t_l [s]
t_v	time period during which the heating surface is covered with a bubble [s]
$\overline{t_v}$	average value of t_v [s]
x	distance from the heating surface [m].

Greek symbols

α	heat transfer coefficient [$W\ m^{-2}\ K^{-1}$]
α_l	heat transfer coefficient due to sensible heat transport, $q_l/\Delta T_{sat}$ [$W\ m^{-2}\ K^{-1}$]
α_v	heat transfer coefficient due to latent heat transport, $q_v/\Delta T_{sat}$ [$W\ m^{-2}\ K^{-1}$]
δ	thickness of liquid film [m]
δ'	thickness of thermal boundary layer [m]
θ	inclination angle of heating surface measured from the horizontal plane [deg.]
λ	thermal conductivity [$W\ m^{-1}\ K^{-1}$].

nucleate boiling from a heating surface facing downwards, where the effect of surface orientation is remarkable, is proposed and the mechanism of heat transfer is discussed quantitatively.

2. EXPERIMENTAL APPARATUS AND PROCEDURE

The experimental apparatus and the location of the heating surface are shown in Fig. 1(a). The heating surface assembly ⑩ is installed in the middle of the inner boiling vessel ② by horizontal supporting tubes ⑪, which pass throughout the inner and outer vessels. These supporting tubes can be rotated around the horizontal axis to position the heating surface in the desired orientation. They are also used to bring power leads and thermocouple leads to and from the inner vessel. By virtue of this supporting structure, the same heating surface can be tested in various orientations, keeping the other factors affecting nucleate boiling, especially surface conditions among them, constant. The inner vessel is surrounded by the outer vessel ③ which serves to keep the system at saturation temperature. Both vessels are equipped with observation windows at the four side walls. Auxiliary electric heaters ⑧ and ⑨ are equipped in both vessels. The former is used to maintain the liquid bulk temperature at its saturation temperature during experiments. But the latter is used to raise the test liquid to its saturation temperature and to degas the inner vessel before experiments, and it is switched off during experiments. The vapor generated in both vessels is condensed by condensers ④ and ⑥.

Details of the heating surface assembly are shown in Fig. 1(b). The heating surface is a rectangular copper plate, 175 mm in length and 42 mm in width, surrounded by fins around its periphery so as to reduce heat losses. The fins and heating surface are cut out in unit body to prevent preferential bubble generation at the edge of the heating surface. Two guide plates ⑱ are installed parallel to the longitudinal edges of the heating surface in order to realize one-dimensional (1-D) bubble flow and to neglect the edge effect. The heat flux across the heating surface is supplied by conduction through the copper block from the electric heaters ⑭ in the slits at the opposite end of the block. Twenty-one thermocouples are embedded along the center line of the copper block at seven longitudinal locations at equal intervals of 25 mm, as shown in Fig. 1(b). The small dots on the copper block ⑬ indicate the positions of the thermocouples. Their depths from the heating surface at each location are 5, 13, and 21 mm, respectively. Three thermocouples are located in the inner vessel to measure the bulk liquid temperature at three different vertical positions.

The heat flux is calculated by using the temperature gradient measured by the thermocouples. It agreed well with the heat flux obtained by correcting the power input for heat losses. The heating surface temperature is measured by extrapolating the measured temperature gradient to the surface. Averaged values for seven longitudinal locations are used as the representative values for the heat flux and the heating surface

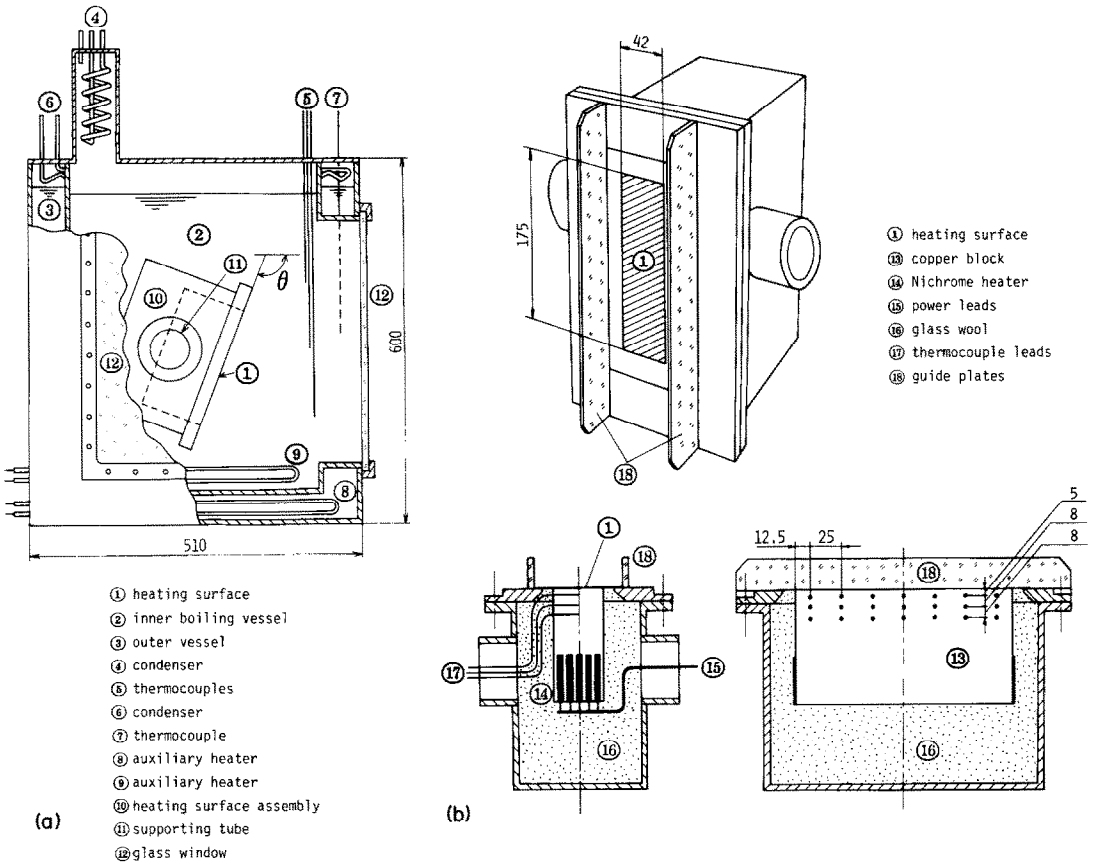

FIG. 1. Experimental apparatus and details of the heating surface assembly.

temperature. And the averaged value for three vertical locations in the liquid is used as the representative temperature of the boiling liquid.

The experiments are performed under the conditions of saturated boiling of distilled water at atmospheric pressure. Before each test run, the heating surface is finished with No. 0/10 emery paper and then rinsed well with ethyl alcohol in an attempt to keep the same surface conditions for all test runs. The heating surface orientation is changed without interrupting the boiling in a series of experiments. Experimental inclination angles measured from the horizontal plane are 0° (a horizontal surface facing upwards), 90° (a vertical surface), 120°, 150°, 165°, and 175° (inclined surfaces facing downwards). Heat transfer measurements were carried out in both processes of increasing heat fluxes and decreasing heat fluxes. But there was no difference between them.

3. EXPERIMENTAL RESULTS

3.1. *Boiling curves and bubble behavior*

The nucleate boiling curves, heat flux q vs temperature difference ΔT_{sat} between the heating surface and the bulk liquid, are shown in Fig. 2(a) for water boiling on the inclined surfaces at atmospheric pressure, where the inclination angle θ is measured from the horizontal plane. An interesting feature of the data presented in Fig. 2(a) is that at low heat fluxes the boiling curves shift upwards with an increase of inclination angle from facing upwards to facing downwards, which are consistent with the previous results by other investigators. However, it is also noteworthy that as heat fluxes are increased the curves seem to merge together into a common boiling curve, although a slight deviation is observed in the opposite direction to that at low heat fluxes. The observed change in the effect of the surface configuration in the range of nucleate boiling region is due to the change in characteristics of bubble behavior and probably also due to the change in the heat transfer mechanism.

Here, with respect to the effect of the surface configuration the nucleate boiling region is subdivided into three regions for convenience of consideration, although at the present time it is not possible to specify the exact location of each region. The first one is the low heat flux region where the effect of orientation appears significantly at heat fluxes less than about 7×10^4 W m^{-2}. The second is the high heat flux region where the effect of orientation disappears at heat fluxes higher than about 17×10^4 W m^{-2}. The third is the middle heat flux region where the effect of orientation

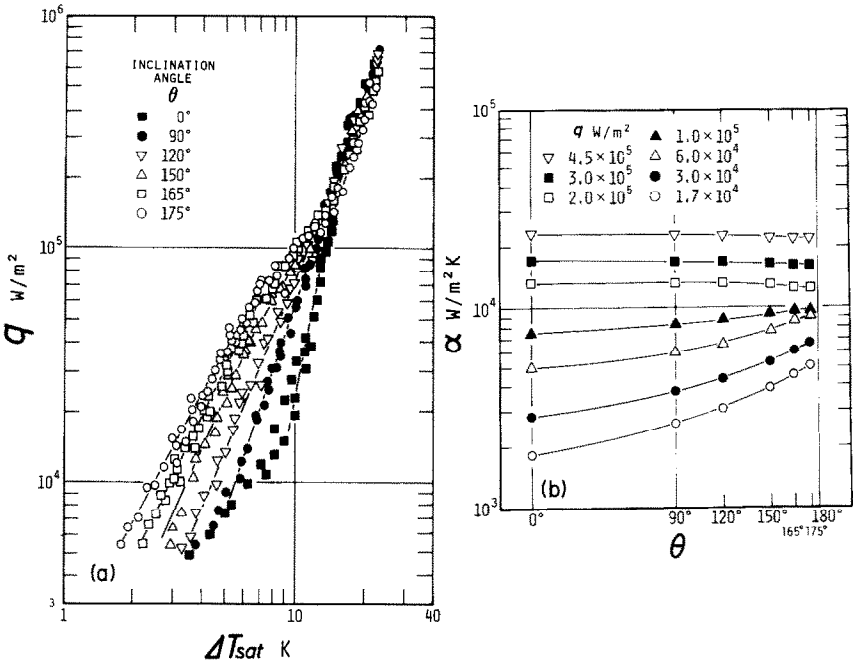

FIG. 2. Effect of surface configuration (experimental results).

disappears asymptotically at heat fluxes between 7×10^4 and 17×10^4 W m^{-2}. Many photographs of bubble behavior along the heating surface were taken from the side and typical results for three regions are shown in Fig. 3. Characteristics of bubble behavior in each region are as follows.

In the low heat flux region, with an increase of inclination angle the population density of nucleation sites on the heating surface decreases and the bubble diameter increases on the contrary. The decrease in nucleation sites is confirmed from observation of the scale deposition at active nucleation sites in the boiling of water containing dissolved nickel salts. For an inclination angle of 0°, bubble generation is almost periodical from the uniformly distributed nucleation sites and a bubble detaches the surface as an isolated bubble. These characteristics hold true up to an inclination angle of 120°. However, for an inclination angle larger than 150° a bubble grows rapidly at the nucleation site immediately after its generation and then the enlarged bubble rises up in the elongated form along the heating surface. As a result the isolated bubbles disappear gradually with an increase of inclination angle. As the heat flux is increased the frequency of bubble generation is increased and enlarged bubbles rise up more periodically.

In the middle heat flux region, even for an inclination angle less than 120° a coalesced bubble begins to appear locally on the heating surface although most of the surface is covered by isolated bubbles. For an inclination angle larger than 150° the clusters of small bubbles begin to be observed between the enlarged bubbles. Thus small bubbles are recognized to coexist together with large bubbles in this region.

In the high heat flux region, bubble generation is so vigorous that coalesced bubbles prevail all over the heating surface for any inclination angle. Especially for an inclination angle larger than 150° a large elongated bubble is produced continuously and covers almost the whole heating surface. The surface of the elongated bubble pulsates irregularly, showing that the vigorous supply of vapor is from the base of the bubble.

3.2. *Effect of surface orientation*

The heat transfer coefficient α is plotted against the inclination angle θ for selected heat fluxes in Fig. 2(b). As seen from the boiling curves in Fig. 2(a) and also evident from Fig. 2(b), with an increase of inclination angle in this range of the experiment the heat transfer coefficient increases at low heat fluxes, while it is almost constant at high heat fluxes independent of inclination angle. Provided that the inclination angle is further increased larger than 175°, the heat transfer coefficient will drop rapidly to a certain minimum value because bubble movement is then completely impeded. This characteristic has been observed also in refs. [4, 8, 9].

The effect of surface configuration is not uniform over the whole region of nucleate boiling. This is perhaps caused by a change in heat transfer mechanisms between low heat fluxes and high heat fluxes. From visual observations of boiling behavior, the relationship between the effect of surface configuration and the heat transfer mechanisms in two regions of low heat fluxes and high heat fluxes is inferred as follows.

In the low heat flux region, for an inclination angle less than 120° heat transfer is mainly controlled by the stirring action of isolated bubbles. As a consequence,

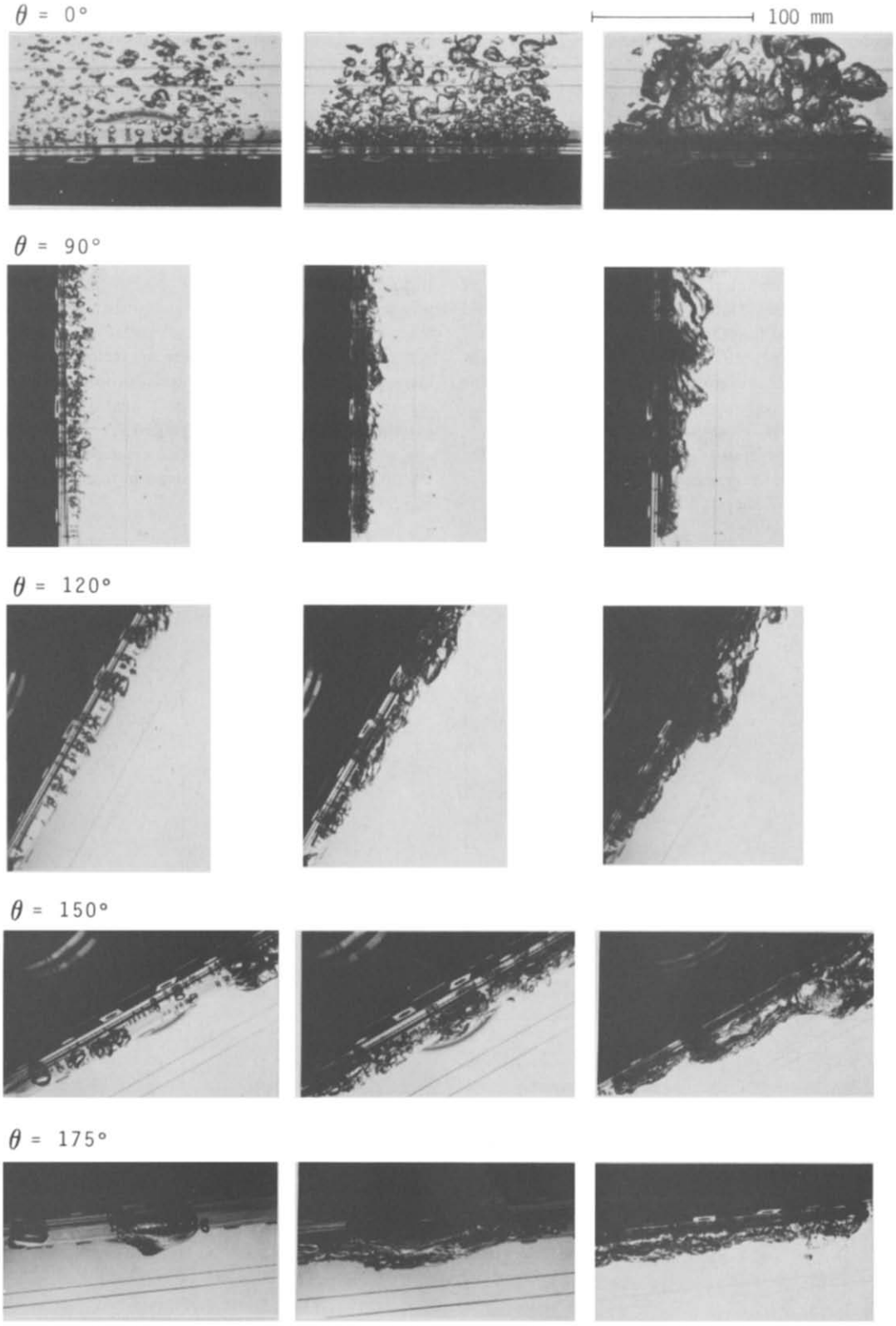

FIG. 3. Photographs of bubble behavior along the surface.

the heat transfer coefficient becomes large when the population density of the nucleation sites is increased in so far as isolated bubbles prevail over the heating surface. However, for an inclination angle larger than 150° heat transfer seems to be controlled by the following two mechanisms because of the appearance of large elongated bubbles and their movement. One is the sensible heat transport by the compulsory removal of the superheated thermal layer from the surface at the time when the elongated bubble rises up along the surface. The other is the latent heat transport by the evaporation of the liquid film underneath the bubble at the time when the surface is covered with the elongated bubble. Provided that these two mechanisms hold true, the heat transfer coefficient does not depend on the number of nucleation sites on the surface and also the nucleation characteristics of the surface.

In the high heat flux region, the flow conditions in the vicinity of the heating surface become important for heat transfer and the generation and movement of large elongated bubbles do not play a role in heat transfer on the contrary to the low heat flux region. Since nucleation in the liquid film under a coalesced bubble controls the flow conditions in the vicinity of the surface, nucleation characteristics of the surface seem to affect heat transfer in this high heat flux region independently of inclination angle.

To confirm the above consideration, the effect of surface orientation is measured for a smooth surface finished with No. 0/10 emery paper and a rough surface finished with No. 0 emery paper, which have different nucleation characteristics. The boiling curves for two surfaces are shown in Fig. 4. For an inclination angle less than 120° the rough surface gives a higher heat transfer coefficient than the smooth one as known generally. On the contrary, for an inclination angle larger than 150° this holds true only in the high heat flux region and there is no difference in heat transfer in the low heat flux region, as expected from the above consideration. These results are considered to support the above idea on the mechanisms in nucleate boiling from the inclined surface.

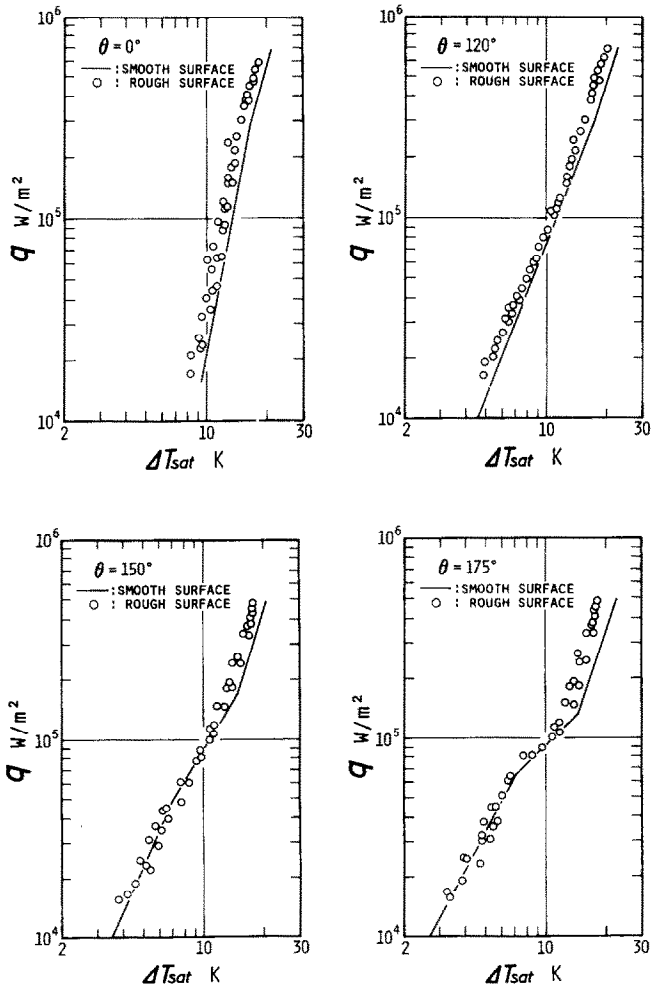

FIG. 4. Effect of surface roughness on heat transfer.

4. HEAT TRANSFER MODEL FOR SURFACE FACING DOWNWARDS

4.1. *Theoretical approach*

The heat flux from a surface facing downwards in the low heat flux region is assumed to be transferred by two mechanisms of the sensible heat transport and the latent heat transport. In the subsequent analysis it is assumed that a rising elongated bubble carries away the superheated thermal layer in front of it. The sensible heat removed in this manner is calculated based on transient heat conduction from the heating surface to the liquid during the liquid period t_l, defined as the time interval during which the heating surface contacts with the bulk liquid. After the liquid period elapses the next bubble rises up and reaches the surface in question. When the bubble passes over the surface the thin liquid film underneath the bubble is evaporated. The latent heat removed in this manner is also calculated by transient heat conduction through the thin liquid film during the vapor period t_v, defined as the time interval during which the heating surface is covered with a rising bubble.

4.1.1. *Sensible heat transport.* Provided that after the thermal layer has been completely carried away by the rising bubble the bulk liquid at saturation temperature T_{sat} comes in contact with the heating surface with constant temperature T_w, then as shown in Fig. 5(a) the boundary and initial conditions for 1-D heat conduction from the surface to the bulk liquid are

$$\begin{aligned} x = 0: &\quad T = T_w \\ x = \infty: &\quad T = T_{sat} \\ t = 0: &\quad T = T_w \quad \text{at } x = 0 \\ &\quad T = T_{sat} \quad \text{at } x > 0 \end{aligned}$$

where x is the distance measured from the surface into the bulk liquid. Then the time-averaged heat flux q_l and heat transfer coefficient α_l during the liquid period t_l are

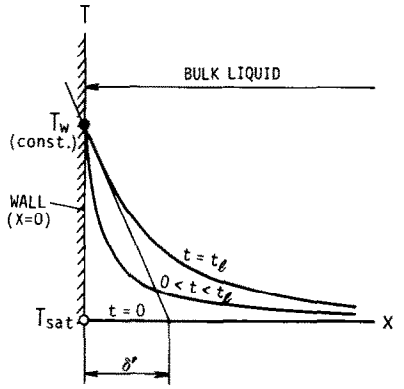

(a) liquid period

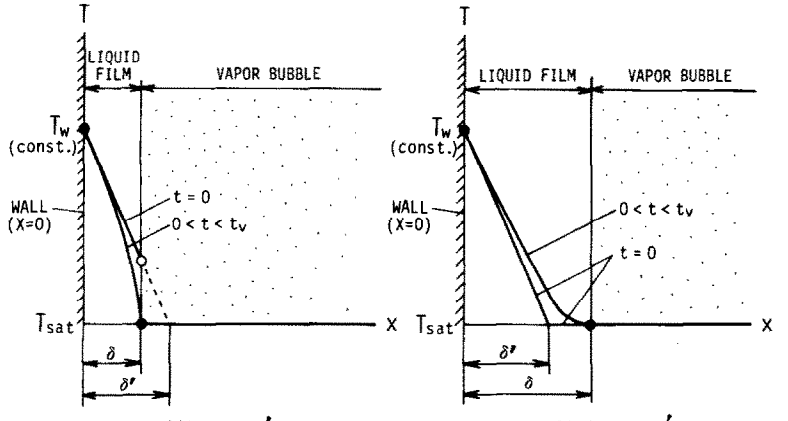

(b) vapor period

FIG. 5. Change in temperature profile near the heating surface during the liquid and vapor period.

obtained as

$$q_l = \frac{1}{t_l}\int_0^{t_l}\left(-\lambda\left.\frac{dT}{dx}\right|_{x=0}\right)dt = \frac{2\lambda\Delta T_{sat}}{\sqrt{(\pi a t_l)}} \quad (1)$$

$$\alpha_l = q_l/\Delta T_{sat} \quad (2)$$

where λ and a are the thermal conductivity and the thermal diffusivity of liquid, respectively, and ΔT_{sat} is the temperature difference between the heating surface and the bulk liquid. The change of temperature profile during the liquid period is outlined in Fig. 5(a).

4.1.2. *Latent heat transport.* When the ascending bubble carries away the bulk liquid in contact with the surface, it is assumed that the thin liquid film remains underneath the bubble and that the temperature profile in this film becomes the initial conditions for conduction during the vapor period, which is approximated in a linear profile as shown in Fig. 5(b). Then the boundary and initial conditions are as follows.

(1) When the liquid film is thinner than the thickness of the thermal layer formed at the end of the liquid period

$$x = 0: \quad T = T_w$$
$$x = \delta: \quad T = T_{sat}$$
$$t = 0: \quad T = T_w - \Delta T_{sat} x/\sqrt{(\pi a t_l)}.$$

(2) When the liquid film is thicker than the thickness of the thermal layer formed at the end of the liquid period

$$x = 0: \quad T = T_w$$
$$x = \delta: \quad T = T_{sat}$$
$$t = 0: \quad T = T_w - \Delta T_{sat} x/\sqrt{(\pi a t_l)} \quad \text{for } x < \delta'$$
$$T = T_{sat} \quad \text{for } \delta' < x < \delta$$

where δ is the liquid film thickness, and δ' is the thickness of the thermal boundary layer defined in Fig. 5(b). Then the time-averaged heat flux q_v and heat transfer coefficient α_v during the vapor period are obtained as

$$(1)\ q_v = \frac{1}{t_v}\int_0^{t_v}\left(-\lambda\left.\frac{dT}{dx}\right|_{x=0}\right)dt$$
$$= \frac{\lambda\Delta T_{sat}}{\delta}\left[1+\frac{2}{t_v}\left(1-\frac{\delta}{\sqrt{(\pi a t_l)}}\right)\right.$$
$$\left.\times\sum_{n=1}^{\infty}\left(-\frac{\delta^2\cos n\pi}{an^2\pi^2}\right)\left\{\exp\left(-\frac{an^2\pi^2}{\delta^2}t_v\right)-1\right\}\right] \quad (3a)$$

$$(2)\ q_v = \frac{\lambda\Delta T_{sat}}{\delta}\left[1-2\sum_{n=1}^{\infty}\left\{\frac{1}{\sqrt{(\pi a t_l)}}\right.\right.$$
$$\times\left(\delta'\cos\frac{n\pi\delta'}{\delta}-\frac{\delta}{n\pi}\sin\frac{n\pi\delta'}{\delta}\right)-\cos\frac{n\pi\delta'}{\delta}\Big\}$$
$$\left.\times\left(-\frac{\delta^2}{an^2\pi^2}\right)\left\{\exp\left(-\frac{an^2\pi^2}{\delta^2}t_v\right)-1\right\}\right] \quad (3b)$$

$$\alpha_v = q_v/\Delta T_{sat}. \quad (4)$$

In order to evaluate heat fluxes q_l due to sensible heat transport and q_v due to latent heat transport, two periods of t_l and t_v and liquid film thickness underneath the elongated bubble are necessary.

4.2. *Liquid and vapor period*

Periods during which the heating surface is in contact with the bulk liquid or covered with a large bubble are measured 0.5 mm above the center of the heating surface using an electric probe which detects liquid phase and vapor phase. If the bubble and the liquid move at the same velocity in the vicinity of the heating surface, then the following time ratio of measured vapor periods to total measured periods gives a void fraction

$$f = \frac{\Sigma t_v}{\Sigma t_l + \Sigma t_v}. \quad (5)$$

Figure 6 shows the void fraction obtained in this way. It increases with an increase of inclination angle and heat flux.

The measured periods t_l and t_v are distributed so widely that the data are treated statistically to find their distribution characteristics. All measured periods are grouped into m class intervals and the number of data in the kth class is termed n_k and the kth class midpoint is termed t_k. Then the ratio of the sum of periods in the kth class to the total periods in all classes gives a frequency

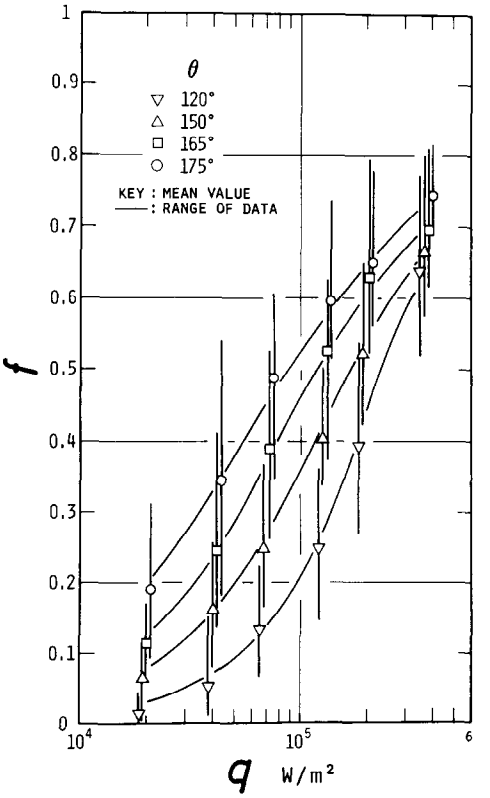

FIG. 6. Void fraction 0.5 mm above the surface.

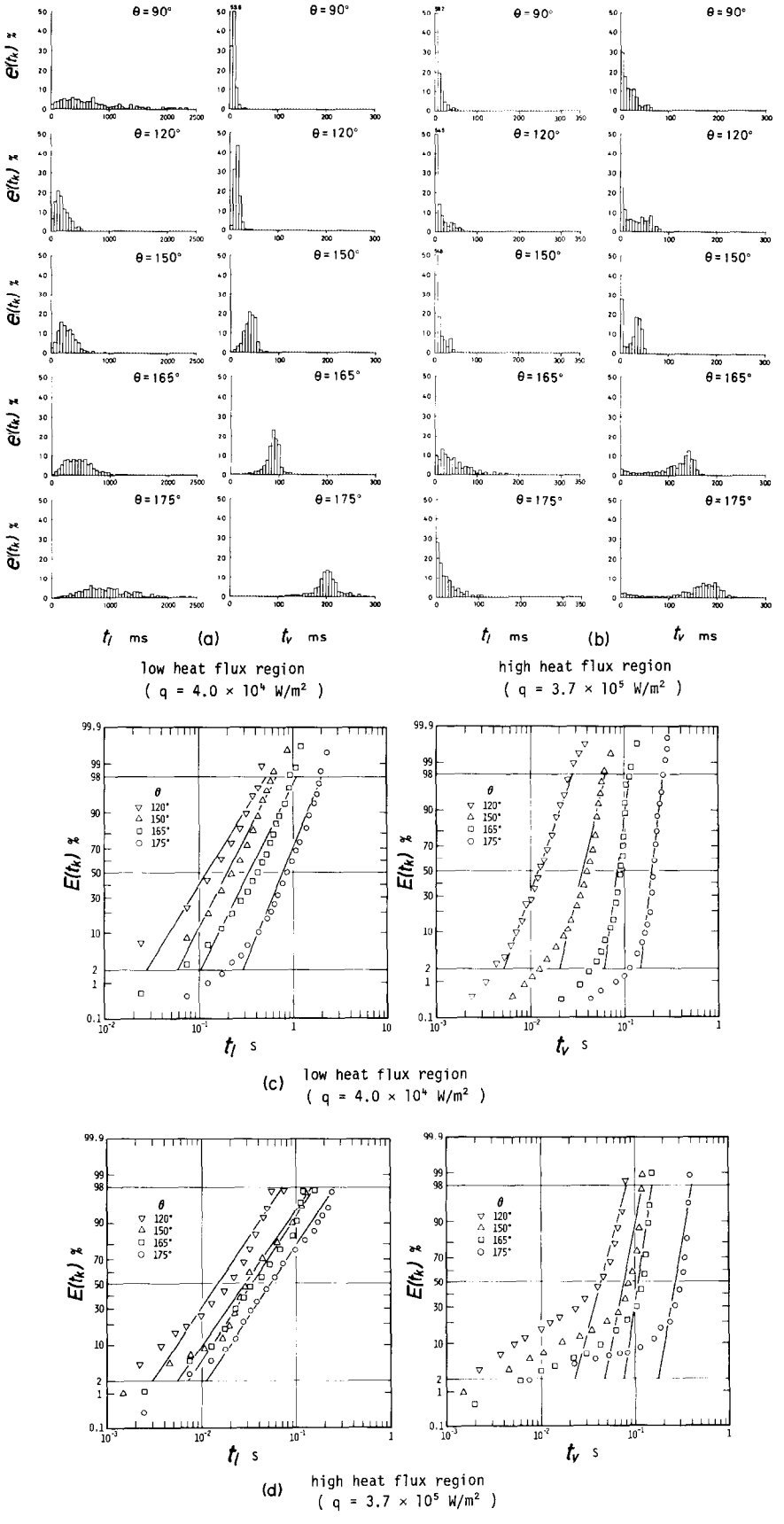

FIG. 7. Distributions of measured liquid and vapor period.

of the period in the kth class [10]

$$e(t_k) = t_k n_k \Big/ \sum_{i=1}^{m} (t_i n_i). \tag{6}$$

Figures 7(a) and (b) show typical patterns of these distributions of t_l and t_v. And the corresponding cumulative frequency is

$$E(t_k) = \sum_{i=1}^{k} e(t_i) = \sum_{i=1}^{k} (t_i n_i) \Big/ \sum_{i=1}^{m} (t_i n_i). \tag{7}$$

Figures 7(c) and (d) show examples of the cumulative distribution curves for t_l and t_v on the logarithmic probability papers. As the curves form the straight lines with the exception of t_v at high heat flux, $e(t_l)$ and $e(t_v)$ obey a logarithmic normal distribution. In the low heat flux region, with an increase of inclination angle both periods t_l and t_v become longer and are distributed over a narrower range. This corresponds to when large bubbles rise up along the surface with a more regular period as the inclination angle is increased. In the high heat flux region, the distribution curve for t_v is composed of two straight lines, which indicates coexistence of large bubbles and small bubbles as confirmed in the photographs.

The average periods $\overline{t_l}$ and $\overline{t_v}$ are determined from Fig. 7 using a logarithmic normal distribution. In evaluating $\overline{t_v}$ in the high heat flux region the straight line through the data points with the longer period is used because the larger bubbles are contributing to heat transfer. Figure 8 shows the average periods $\overline{t_l}$ and $\overline{t_v}$.

The rising frequency of bubbles is given by the inverse of the sum of the liquid and vapor period. It is clear from Fig. 8 that the rising frequency decreases with an increase of inclination angle and it becomes extremely high in the high heat flux region, which indicates the occurrence of vigorous boiling.

4.3. *Liquid film thickness*

As it is difficult to measure the liquid film thickness beneath the vapor bubble rising up along the heating surface, measurements are performed here for a liquid film formed between the non-heating surface and the air bubble rising along it. The results are assumed to be applicable to the case of a boiling bubble.

A pair of electrodes 1 mm in diameter is embedded in an acrylic plate at a distance of 4 mm apart. The electric resistance between the electrodes is measured when the injected air bubble passes over them [11]. Then the film thickness is determined from the calibration curve between the electric resistance and the film thickness. Figure 9 shows the calibration apparatus. Injected air bubbles have volumes of 2, 4, and 8 cm^3. And injection frequency is varied. But bubble size and frequency have no appreciable effect on the measured results. The measured film thickness is given in Table 1.

4.4. *Results of analysis*

Equations (1)–(4) are evaluated by substitution of measured data on the liquid period $\overline{t_l}$, the vapor period $\overline{t_v}$, the film thickness δ, and the temperature difference ΔT_{sat}. Figures 10(a) and (b) show the heat transfer coefficients α_l when the heating surface is in contact with the bulk liquid, and α_v when the heating surface is covered by large bubbles. As is evident from the figures, the effect of inclination angle is large in α_v, while α_l is rather insensitive to the variation of inclination angle. Thus the observed effect of surface configuration on heat transfer is concluded to be mainly due to latent

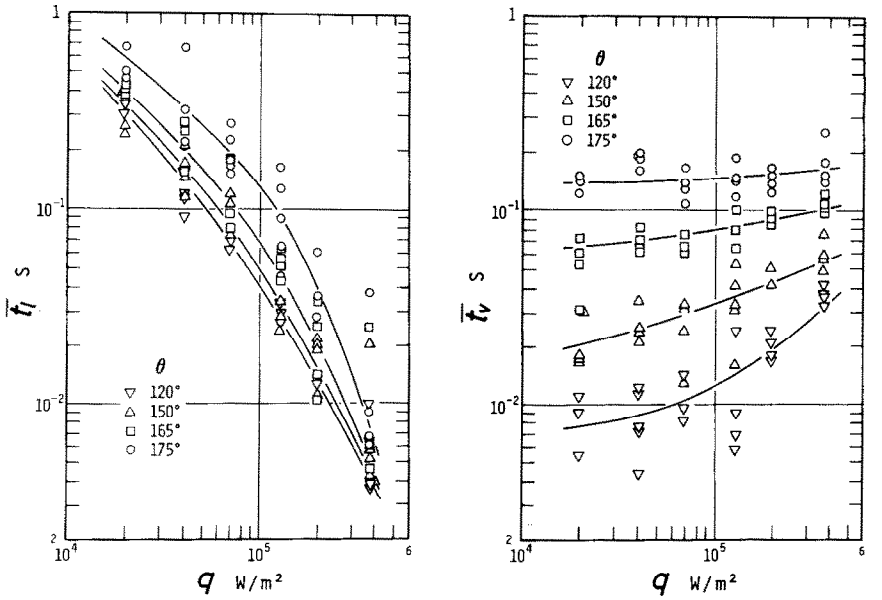

FIG. 8. Average liquid period and average vapor period.

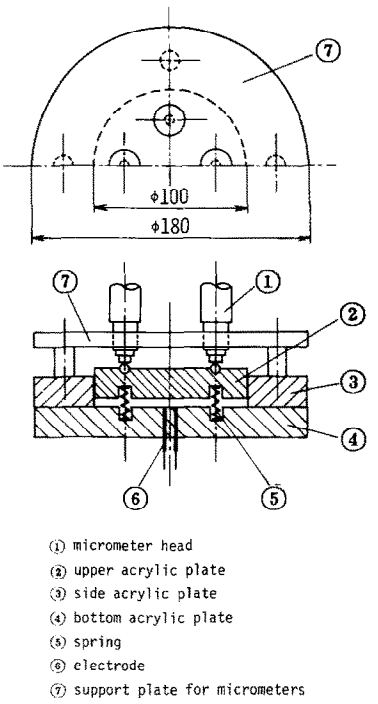

FIG. 9. Calibration apparatus for relation between electrical resistance and film thickness.

Table 1. Liquid film thickness formed beneath air bubble

Inclination angle θ (deg.)	Thickness of liquid film (μm)		
	Max.	Av.	Min.
120	473	401	273
150	178	145	112
165	101	78	53
175	64	44	24

Experimental conditions: electric conductivity of water, 6200 ~ 49 600 Ω cm; volume of air bubble, 2, 4, 8 cm^3.

heat transport from the surface to the rising elongated bubble.

As the heating surface is alternatively in contact with the bulk liquid and the rising bubble, the time-averaged heat flux q_c can be expressed in terms of q_l, q_v and f as follows

$$q_c = (1-f)q_l + fq_v. \tag{8}$$

The first term on the RHS represents the contribution of sensible heat transport and the second term to that of latent heat transport. Figure 10(c) shows the contribution of latent heat transport relative to the

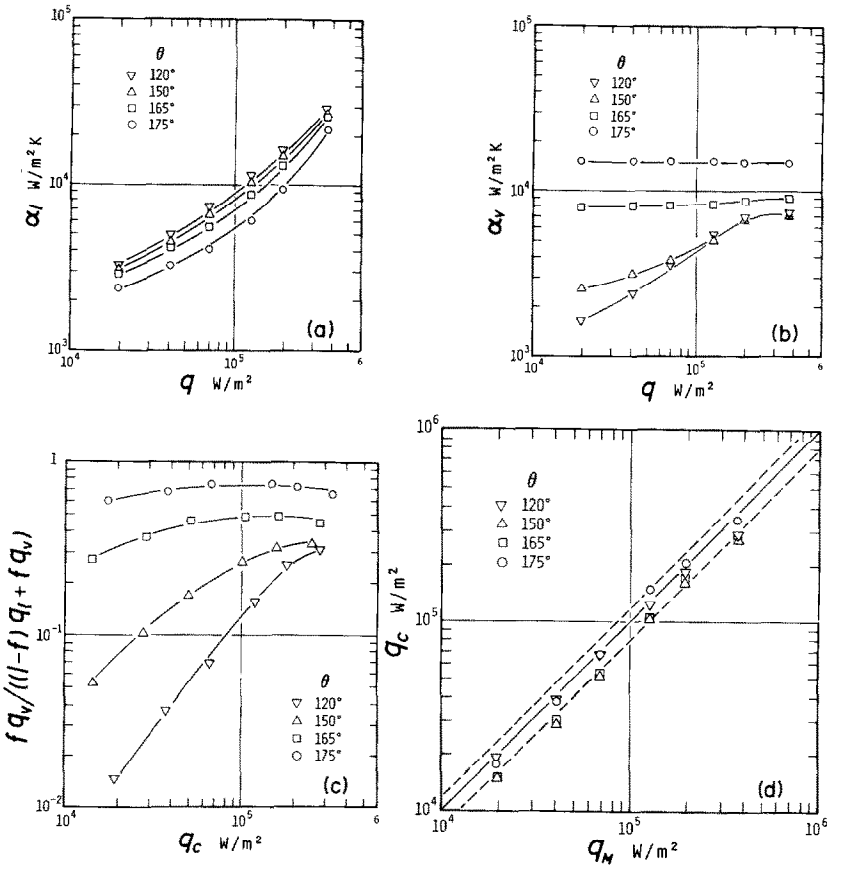

FIG. 10. Results of calculation based on proposed model for heat transfer.

total heat transport. This contribution becomes more predominant at larger inclination angles.

The calculated heat flux q_c is compared with the measured one q_M in Fig. 10(d). Good agreement supports the present theoretical approach on the mechanism of heat transfer from the heating surface facing downwards.

5. CONCLUSION

In order to clarify the effect of the surface configuration on nucleate boiling heat transfer, the experiments were carried out for the saturated pool boiling of water at atmospheric pressure. The inclination angle of a rectangular heating surface was varied from 0° to 175°. The experimental results show that the effect of the surface configuration is remarkable at low heat fluxes and the heat transfer coefficient becomes large as the inclination angle is increased in this case, while no marked effect is observed at high heat fluxes.

Two mechanisms are considered to concern heat transfer from the inclined surface facing downwards. One is the sensible heat transport due to compulsory removal of the thermal layer by the elongated bubble rising along the surface. The other is the latent heat transport due to evaporation of the thin liquid film beneath the elongated bubble. The analytical model of these mechanisms indicated that the heat transfer from the inclined surface facing downwards is controlled mainly by the latent heat transport.

REFERENCES

1. K. Nishikawa, Y. Fujita, M. Tsutsui and K. Yoshimoto, On the nucleate boiling heat transfer from the vertical surface, *Proc. 13th National Heat Transfer Symp. Japan*, pp. 394–396 (1976).
2. K. Nishikawa, Y. Fujita, M. Tsutsui and T. Ono, On the nucleate boiling heat transfer from the vertical surface (further report), *Proc. 16th National Heat Transfer Symp. Japan*, pp. 295–297 (1979).
3. M. Jakob und W. Linke, Der Wärmeübergang beim Verdampfen von Flüssigkeiten an senkrechten und waagerechten Flächen, *Phys. Z.* **36**(8), 267–280 (1935).
4. P. M. Githinji and R. H. Sabersky, Some effects of the orientation of the heating surface in nucleate boiling, *Trans. Am. Soc. Mech. Engrs*, Series C, *J. Heat Transfer* **85**(4), 379 (1963).
5. B. D. Marcus and D. Dropkin, The effect of surface configuration on nucleate boiling heat transfer, *Int. J. Heat Mass Transfer* **6**, 863–866 (1963).
6. C. R. Class, J. R. Dehaan, M. Piccone and R. B. Cost, Boiling heat transfer to liquid hydrogen from flat surfaces, *Adv. Cryogen. Engng* **5**, 254–261 (1959).
7. J. W. Littles and H. A. Wallis, Nucleate pool boiling of Freon 113 at reduced gravity levels, ASME paper, 70-HT-17 (1970).
8. L. T. Chen, Heat transfer to pool-boiling Freon from inclined heating plate, *Lett. Heat Mass Transfer* **5**(2), 111–120 (1978).
9. I. P. Vishnev, I. A. Filatov, Ya. G. Vinokur, V. V. Gorokhov and G. G. Svalov, Study of heat transfer in boiling of helium on surfaces with various orientations, *Heat Transfer—Sov. Res.* **8**(4), 104–108 (1976).
10. Y. Iida, Research on the estimation of flow pattern in the two-phase flow of vapor and liquid, *Trans. Jap. Soc. Mech. Engrs* **45**(394), 895–903 (1979).
11. G. F. Hewitt, R. D. King and P. C. Lovegrove, Technique for liquid film and pressure drop studies in annular two-phase flow, AERE-R 3921 (1962).

EFFET DE LA CONFIGURATION DE LA SURFACE SUR LE TRANSFERT THERMIQUE PAR EBULLITION NUCLEEE

Résumé—Pour étudier en détail l'effet de la configuration de la surface sur le transfert thermique par ébullition nucléée, on étudie l'ébullition de l'eau en réservoir, à la pression atmosphérique, sur une plaque plane de cuivre dont l'orientation est variable entre 0° et 175° par rapport à l'horizontale. L'effet de l'inclinaison est remarquable dans la région des faibles flux thermiques et il se traduit par l'augmentation du coefficient de transfert lorsque l'angle augmente. Au contraire il n'y a pas d'effet marqué dans la région des grands flux. Pour expliquer l'effet observé sur des surfaces orientées vers le bas, deux mécanismes sont proposés : le transfert de chaleur sensible par le déplacement de la couche thermique imposé par l'ascension des bulles et par le transfert de chaleur latente dû à l'évaporation du film liquide mince sous la bulle qui monte. La dernière contribution devient prédominante pour les grands angles d'inclinaison.

DER EINFLUSS DER OBERFLÄCHENANORDNUNG AUF DEN WÄRMEÜBERGANG BEI DER BLASENVERDAMPFUNG

Zusammenfassung—Zur ausführlichen Untersuchung des Einflusses der Oberflächenanordnung auf den Wärmeübergang bei der Blasenverdampfung wurde ein Experiment für das Behältersieden bei Atmosphärendruck an einer ebenen Kupferplatte durchgeführt, deren Neigung von 0° bis 175° aus der Waagerechten variiert wurde. Der Einfluß der Oberflächenneigung ist im Bereich niedriger Heizflächenbelastungen bemerkenswert, dabei nimmt der Wärmeübergang mit dem Neigungswinkel zu. Andererseits ist kein ausgeprägter Einfluß im Bereich höherer Heizflächenbelastungen festzustellen. Zur Erklärung des beobachteten Einflusses der Oberflächenneigung bei abwärts gerichteten Oberflächen wurden zwei Mechanismen, des fühlbaren und des latenten Wärmetransports vorgeschlagen : die durch aufsteigende Blasen erzwungene Entfernung der thermischen Grenzschicht und der Transport latenter Wärme durch Verdampfung des dünnen Flüssigkeitsfilms unterhalb der aufsteigenden Blasen. Der letztere Beitrag wird bei großen Neigungswinkeln dominierend.

ВЛИЯНИЕ ПОЛОЖЕНИЯ ПОВЕРХНОСТИ НА ТЕПЛОПЕРЕНОС ПРИ ПУЗЫРЬКОВОМ КИПЕНИИ

Аннотация—Для детального исследования влияния положения поверхности на теплоперенос при пузырьковом кипении проведены эксперименты по пузырьковому кипению воды в открытом объеме при атмосферном давлении на медной плоской пластине, помещаемой под различными углами наклона (от 0° до 175°) к горизонтальному положению. Положение поверхности оказывает существенное влияние в области низких значений теплового потока, в которой коэффициент теплопереноса увеличивается с ростом угла наклона. В области же высоких значений теплового потока заметного влияния не наблюдается. Для объяснения данного эффекта на поверхностях, обращенных лицевой стороной вниз, предложено два механизма переноса тепла: перенос отводом теплового слоя поднимающимися пузырьками и перенос скрытой теплоты испарением из тонкой жидкостной пленки под поднимающимися пузырьками. При больших углах наклона вклад второго механизма становится доминирующим.